Investigation of Ocean Dynamics using Argo Float Data

A Thesis

submitted to
Indian Institute of Science Education and Research Pune
in partial fulfilment of the requirements for the
BS-MS Dual Degree Programme

by

Kashika Singh

Indian Institute of Science Education and Research Pune
Dr. Homi Bhabha Road,
Pashan, Pune 411008, INDIA.

May, 2025

Supervisors: Dr Joy Merwin Monteiro, Prof Jonas Nycander

Certificate

This is to certify that this dissertation entitled Investigation of Ocean Dynamics using Argo Float Datatowards the partial fulfilment of the BS-MS dual degree programme at the Indian Institute of Science Education and Research, Pune represents study/work carried out by Kashika Singh at Indian Institute of Science Education and Research under the joint supervision of Dr Joy Merwin Monteiro, Assistant Professor, Department of Earth and Climate Sciences, IISER, Pune and Prof Jonas Nycander, Professor, Department of Meteorology, Stockholm University during the academic year 2024-2025.

Dr Joy Merwin Monteiro

Prof Jonas Nycander

Dr Suhas Ettammal

Declaration

I hereby declare that the matter embodied in the report entitled "Investigation of Ocean Dynamics using Argo Float Data" are the results of the work carried out by me at the Department of Earth and Climate Sciences, IISER, Pune and the Indian Institute of Science Education and Research, Pune, under the joint supervision of Dr Joy Merwin Monteiro, Department of Earth and Climate Sciences, IISER, Pune and Prof Jonas Nycander, Department of Meteorology, Stockholm University, and the same has not been submitted elsewhere for any other degree.

Kashika Singh

Registration Number: 20201180

This thesis is dedicated to cats everywhere. And coffee, lots of coffee.

Acknowledgements

First and foremost, I would like to thank my supervisors, Prof Jonas Nycander and Dr Joy Monteiro, for their mentoring throughout the thesis. Without their invaluable input and support, none of this would have been possible. I have learnt so much in this short duration, and it's all thanks to them. I would also like to thank Dr Gaspard Geoffroy for answering my innumerable emails about the minutiae of his work, which ultimately helped me so much with my own.

Secondly, I would like to thank my labmates Dilip and Devosmita, who helped me with theory and generally made my time in the lab enjoyable.

I am also extremely grateful for the friends I have made during my time in IISER: Krishna and Pooja, who let me treat their room as mine and were always there for me; Jason, who never failed to make my day better; Asita, Akash and Anshuka, who were always there when I was bored or lonely, Shijil and DP who were there for me throughout the minefield of ECS courses and the many coffee breaks that entailed, Unni and Achintya who helped me with all of my concerns about my thesis, Arjun, for many, many things, and lastly, Marodia who's the reason I met all these wonderful people in the first place.

None of this would have been possible without my parents' continued support; I can't describe how much that means to me.

Last but not least, I would like to thank my emotional support copy of Pedlosky's *Geophysical Fluid Dynamics* that I didn't read much of but had checked out of the library the entire year.

Abstract

Ocean mesoscale eddies are an essential part of the climate system. They are responsible for increasing the primary productivity of the regions they exist in and drive massive amounts of momentum, salinity and nutrient transport. Eddies exist everywhere in the ocean but are more common near energetic currents like the Kuroshio Current and the Antarctic Circumpolar Current. Due to their significant impacts and ubiquity, they are important to study.

Argo floats are instruments that measure the temperature values at a depth of 1000 dbar in the ocean before rising up while measuring the temperature and salinity profiles of the ocean. The data they collect at a depth of 1000 dbar is called park phase data.

The park phase data has not been used extensively as it is only available for some of the Argo floats. However, we used Argo park phase data and the Sea Level Anomaly (SLA) from satellite data along the track of the float to detect eddies. We considered persistent periods of anti-correlation between these curves a sign of eddy activity. We then used the first baroclinic mode to predict the displacement at 1000 dbar depth to compare with the observational displacement time series we get from Argo floats.

We find a good correlation between the observational Argo displacement time series and the SLA time series and between the observational displacement and the displacement predicted by the first baroclinic mode in some cases. This implies that the Argo park phase data can be used to detect eddies by correlating with the SLA and that it can be used to look at the vertical structure of eddies in the ocean.

Contents

List of Figures

Chapter 1

Introduction

Oceanic eddies are large swirling vortices of seawater that are ubiquitous in Earth's oceans. They are so abundant that they can dominate over the effects of the large-scale mean flow on daily Sea Surface Height (SSH) and Temperature (SST) maps.

Though eddies can exist on multiple scales in the oceans, the ones we are interested in are called mesoscale eddies. They are caused by baroclinic instabilities in the fluid. Mesoscale eddies extend from tens to hundreds of kilometres in the horizontal and can last anywhere from a couple of days to a couple of months [1] with some lasting for a year or more. They are responsible for many changes in the regions in which they exist. They transport vast amounts of heat, salinity and momentum, which helps to modulate the Earth's climate system in turn. They can bring cold and nutrient-dense water up to the surface which can then lead to an increase in the primary productivity of the region. They have also been shown to make coral reefs more resilient to temperature extremes caused by climate change by introducing them to a wide range of temperatures [2].

They take away available potential energy from the large-scale mean flow of the ocean and convert it into eddy kinetic energy. They account for most of the kinetic energy variability in the oceans [1].

Before satellite measurements were commonplace, eddies (and other oceanic phenomena) were studied using shipboard measurements, buoys and other scarce, in-situ measurements. While this was good to study a small region of the ocean, it wouldn't suffice for global

studies. After its advent, satellite altimetry has been the preferred method for studying the oceans. Baroclinic eddies are now extensively studied using satellite altimetry, with some studies using in situ measurements from ships and buoys as well. The problem with using altimeter data is that it gives a top 2-dimensional view of the ocean from which the 3-dimensional structure needs to be deciphered. Many attempts have been made to look at the vertical structure of eddies, firstly calculating Empirical Orthogonal Functions (EOFs) [3]. This is impractical to be done everywhere in the oceans as you would require accurate, current readings in all regions and the lowest EOF has been found to be a combination of the barotropic mode and the first baroclinic mode [4]. Due to this, people started looking at the barotropic and baroclinic modes themselves, using the density climatology values as a way to explain the sea surface height and kinetic energy variability [4].

Therefore, while there have been attempts to look at eddies just from the Sea Level Anomaly (SLA, difference between average sea surface height and the actual sea surface height at a given point) fields, to look at them in the vertical with EOFs and Baroclinic modes, they haven't been studied using Argo park phase data as we did in this thesis project. The Argo park phase data give us time series of displacement measured by the float at 1000 dbar (the depth at which Argo floats' park phase occurs). During the park phase, the float has no velocity of its own and freely drifts with the currents; we can get a good record of how these currents alter the isopycnals along which the float is moving. This gives us a unique way to look at mesoscale eddies. We were able to see how they affect the isopycnals at this depth.

We created time series of SLA along the track of several hundred Argo floats and then correlated those with the displacement at 1000 dbar from the Argo park phase data. From this, we can see many clear eddy events recorded in these two time series together. To validate that these were actually eddy events, we calculated the displacement that the same SLA time series would cause if they were associated with the first baroclinic mode. This validated some of the eddies that we found using the SLA time series and the displacement measured by Argo floats. We also used AVISO eddy trajectory data to see the eddies that were flagged by the park phase data and the first baroclinic mode.

In the end, we got a good correlation between the park phase data and the SLA time series for some floats, which were, in turn, nicely validated by displacement predicted by the first baroclinic mode. Analysis of data from more Argo floats is required for more concrete

results.

Contributions of this thesis

- Correlating Argo Park Phase data with SLA time series to detect eddies.
- Solving the Sturm-Liouville Eigenvalue Problem using Argo Vertical Profile data and climatology data.
- Comparing the eddy prediction from the eigenvalue problem to the detected eddies from Argo Park Phase data.
- Comparing tracked eddies from the AVISO data set to the detected eddies.

Chapter 2

Data and Methods

2.1 Data

2.1.1 Argo Floats

Argo floats are freely drifting profiling floats that measure the salinity and temperature profiles of the upper 2000 m of the oceans [5]. They work in cycles of 10 days. During the first nine and a half days, the float drifts freely at a depth of 1000 dbar; this part of the cycle is called the park phase of the Argo float. During this phase, the float collects temperature and pressure data once every hour. After the park phase, the float dives down to a depth of 2000 dbar. Then, it rises rapidly to the surface, collecting the salinity and temperature profiles, concluding one cycle by surfacing and relaying its position and the collected data. We also used the salinity and temperature profiles to look at the associated vertical eigenmodes. Argo floats are mainly designed to record the profile data, but some floats also record the park phase. These are the data that we use most. They have only been used sparingly to examine ocean dynamics at these timescales. They have been used to look into internal tides and their variability [6], [7].

In this thesis, we used preprocessed [7] Argo data. Here, the park phase data of the floats have been used to calculate the vertical isotherm displacement for each time point at 1000 dbar (henceforth known as η). To calculate η, we need the temperature gradient, which is

calculated around 1000 dbar using Argo profile data, $\overline{T}_p$, which is the mean temperature over a cycle, and $T_p(t)$ just denotes the hourly temperature readings.

$$\eta_T(t) = \frac{T_p(t) - \overline{T}_p}{(dT/dP)_{1000}} \tag{2.1}$$

This equation would usually be enough to calculate the vertical isotherm displacement at a particular depth, but due to the fact that Argo floats are not entirely isobaric in nature and frequently have small departures from 1000 dbar, we need to introduce a correction term, η_P.

$$\eta_P(t) = \overline{P}_p - P_p(t) \tag{2.2}$$

Here, $\overline{P}_p$ is the mean pressure over one cycle, and $P_p(t)$ represents the hourly pressure measurements. Now, the vertical isothermal displacement can be calculated.

$$\eta(t) = \eta_T(t) - \eta_P(t) \tag{2.3}$$

This calculation of η holds only for η variations at time scales lower than the length of one cycle. However, mesoscale eddies usually exist at much longer time scales. We need another correction term, $d\eta$, to reintroduce the low-frequency variability in η. The $d\eta$ term is again calculated by first calculating $d\eta_T$ and $d\eta_P$ and then putting them together. Here, $d\eta_T$ is calculated by dividing the difference of the average temperature of two consecutive cycles by the temperature gradient at 1000 dbar and $d\eta_P$ is the difference between the average pressure between two consecutive cycles. Finally, the vertical displacement of isotherms is calculated by adding the hourly η and $d\eta$ time series.

2.1.2 Satellite Altimetry Data

In this thesis, we used a gridded satellite product with a daily resolution of $0.25° \times 0.25°$ from the Copernicus Marine Service to get the sea surface height above Sea Level (SLA(m)). In Fig 2.1, we can see the time-averaged SLA(m) in an area around the track of an Argo Float over its entire life cycle.

This study has been conducted using E.U. Copernicus Marine Service Information; https://doi.org/10.48670/moi-00145.

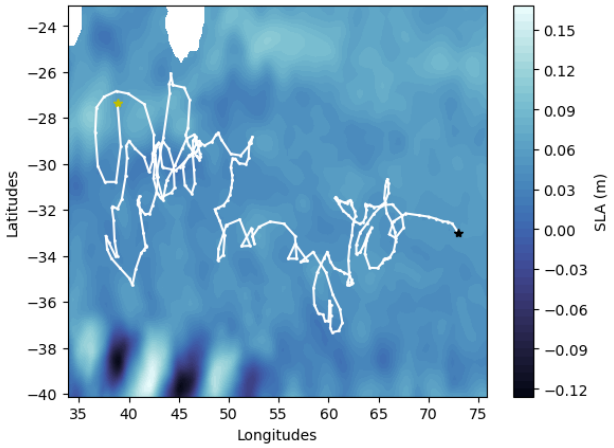

Figure 2.1: The track of Argo Float 1900411 (World Meteorological Organization (WMO) Identification) superimposed onto the time-averaged SLA(m) over the lifetime of the float.

2.1.3 Global Eddy Trajectory Data

From Archiving, Validation and Interpretation of Satellite Oceanographic data (AVISO), we used the Mesoscale Eddy Trajectories Atlas (META3.2 DT) dataset. This data set provides eddy trajectories, contours and amplitudes derived from satellite altimetry for our entire study period, daily. The altimetric Mesoscale Eddy Trajectories Atlas was produced by SSALTO/DUACS and distributed by AVISO+ (https://aviso.altimetry.fr) with support from Centre national d'études spatiales (CNES), in collaboration with The Mediterranean Institute for Advanced Studies(IMEDEA) (DOI:10.24400/527896/a01-2022.006)

2.1.4 World Ocean Atlas Climatology Data

The annual climatological values for the temperature and salinity profiles from the World Ocean Atlas (WOA) (doi: 10.25921/va26-hv25) were used to extend the Argo temperature and salinity profiles to the bottom. This was necessary as the Argo floats only profile the upper 2 km of the ocean. To accurately calculate the vertical eigenmodes, these profiles must be extended to the bottom of the basin. These profiles were then re-gridded to an evenly spaced grid for calculation purposes. We used annual climatologies over seasonal climatologies for this purpose, as they usually have more resolution than their seasonal counterparts. The climatological profiles are not significantly different in the deep ocean ($>$ 2000 dbar) from the seasonal to annual values [8].

2.1.5 Bathymetry Data

The global ocean bathymetry data were obtained from the General Bathymetric Chart of the Oceans (GEBCO). This data set contains ocean bathymetry data at a $0.25° \times 0.25°$ resolution. We converted this to a resolution of 5° later. We used this to accurately determine the depth until which the altered profiles from Section 2.1.4 should be extended. In cases where the last values of depths of the altered profiles are less than the depth of the bathymetry, we repeat the last value of temperature (or salinity) until we reach the bottom. This data set is from GEBCO Compilation Group (2024) GEBCO 2024 Grid (doi:10.5285/1c44ce99-0a0d-5f4f-e063-7086abc0ea0f).

2.2 Methods

2.2.1 Argo Data Selection

We had data from 2092 Argo floats, but most of these data were not used. The criteria for selection are as follows:

1. The float had data for more than 2 months.
2. The float had 10-day cycles.

The first criterion is necessary, as it would become increasingly more challenging to study mesoscale eddies with time periods shorter than 2 months. The second criterion stems from the fact that there are some floats that operate on 5-day cycles. The data from these floats is not usable after applying a designed low-pass filter (explained more in Section 2.2.2). Only 339 floats satisfied these criteria.

2.2.2 Finite Impulse Response Filter

The η time series of the Argo floats is largely dominated by tidal signals (at both semidiurnal and diurnal tidal frequencies). Since the eddies occur at much lower frequencies

(with timescales ranging from a couple of days to a couple of months or more), we needed to filter out the tidal contribution to the total signal. This was done using a low-pass Finite Impulse Response (FIR) filter with a cut-off frequency of 4 days, which was applied using a *Hann* window. Henceforth, any mentions of the η time series refer to the filtered η time series. We chose an FIR filter as that would grant us the most control over the shape and size of the filter so that we could specifically target certain frequencies to attenuate.

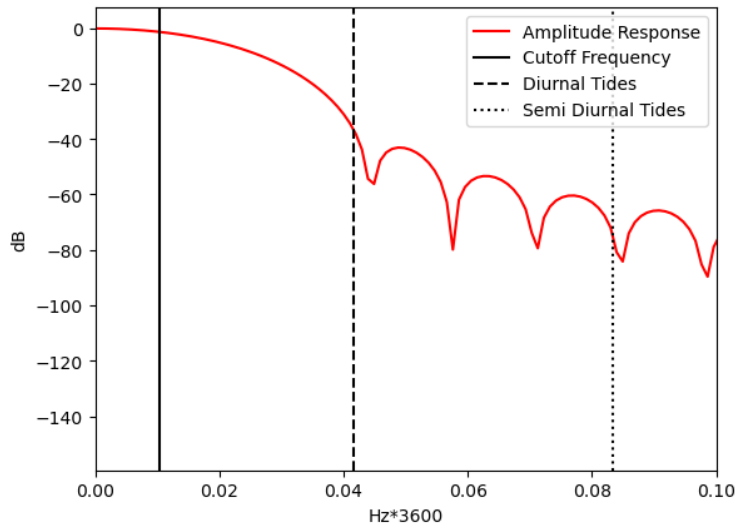

Figure 2.2: The amplitude response of the FIR filter.

In Fig 2.2, we have the amplitude response of the FIR filter we created. This shows us which frequencies were subdued and by how much. The passband of the filter, the frequencies in this region would pass without attenuation, extends from zero till the cut-off frequency. It is a part of the main lobe which extends till the first trough in the curve. This is then followed by the stop band of the filter, where you get many side lobes which control the amount of attenuation you get at different points in the stop band.

We looked into the power spectra of the η time series produced by the Argo floats and found that the tidal frequencies were many orders of magnitudes more powerful than the lower frequency eddy activity. Since the purpose of the filter was to subdue the effect of tidal activity on the η time series specifically, both tidal frequencies fall into troughs in the stop band of the amplitude response (Fig 2.2). This ensures that the tidal frequencies are especially attenuated to account for their higher amplitude in the power spectra.

As is evident in Fig. 2.3, the length of the filtered η time series is much shorter than that

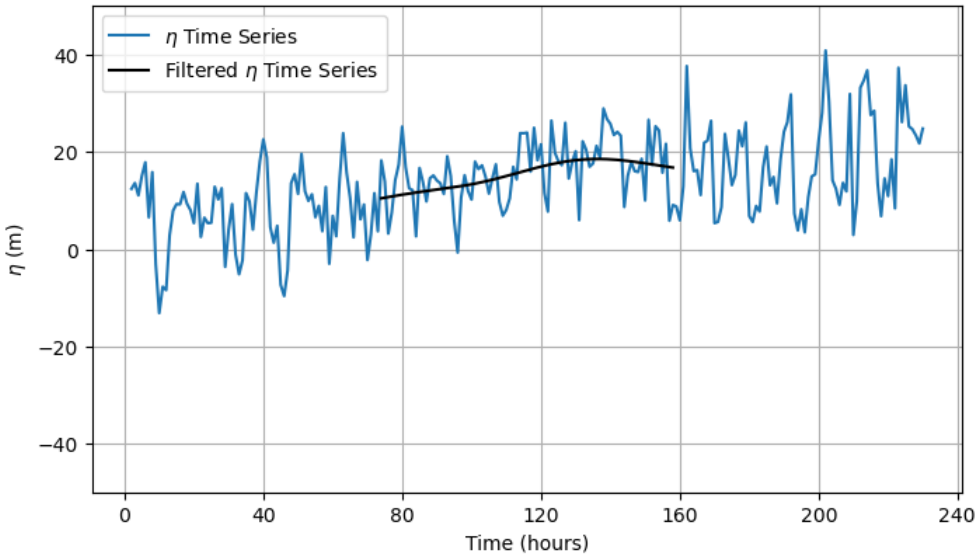

Figure 2.3: The filtered and unfiltered η time series for float 1900411 (WMO) in the Indian Ocean for the first cycle of the float.

of the unfiltered version. This is because the FIR filter only produces values when the entire width of the filter receives valid values. Therefore, as each of the cycles have a couple of invalid values on either sides (due to the profiling part of a typical Argo float cycle), there is data missing from both sides. The length of the missing data is equal to the number of filter weights on both sides. This means that we lose about half of our data for each cycle. This still leaves us with enough data left over to see the patterns of isopycnal displacement caused by eddy activity, as many mesoscale eddies last for timescales much longer than a single cycle of an Argo Float. Therefore, putting a few cycles of an Argo float in addition to the SLA time series along the float track can help us reconstruct the correlation between the surface and the interior of the ocean at that point.

2.2.3 Creating Daily SLA Time Series

We needed a daily SLA time series so we could compare the surface SLA to η. This helped in visualising whether there was an eddy passing along the track of the float at a particular time.

To get the daily SLA time series, we needed to know the positions of the float daily. However, the positions of the Argo floats are known only at the end of a cycle, i.e. once

every 10 days. To approximate the daily positions of the Argo floats, we linearly interpolated the positions of the float between two successive cycles of the float. The values of η are known on an hourly basis, and the values of SLA(m) (from satellite altimetry data) are known daily at midnight UTC. So, in order to make two coherent and comparable time series, we only took the values of η at midnight into consideration.

Since the satellite data is available only on a regular grid, we needed to calculate the weighted average of the SLA(m) (weighted by the distance of the grid point from the float) at the four grid points enclosing the float position at a time point, to get the SLA at the interpolated positions of the float. This allowed us to create a daily time series for SLA based on the interpolated daily float positions.

2.2.4 Correlating the Surface and the Interior

Eddies exist in two broad classes; there are eddies that depress the surface of the ocean and bring up the isopycnals in the interior (Cyclonic eddies), and there are eddies that elevate the surface and push down on the isopycnals in the interior (Anti-cyclonic eddies). We can see this when we correlate the SLA and the η time series in Section 3.1, but to validate our findings, we calculated the vertical baroclinic modes from the stratification profiles. From the eigenmodes, we calculated the ratio of the displacement of the surface to displacement at 1000 dbar. This ratio is what we needed to be able to predict the amount of displacement at 1000 dbar with only the SLA time series.

Calculating Eigenfunctions

To compare the surface displacement of the ocean (in terms of the SLA) to the vertical displacement of isopycnals at a designated depth (which is 1000 dbar in our case), we used the linear quasi-geostrophic potential vorticity (QGPV) equation [9]. Here, the surface displacement and η can be directly related to each other by the Brunt–Väisälä frequency, N^2.

The Brunt–Väisälä frequency was calculated using the temperature and salinity profiles from Sections 2.1.4 and 2.1.5 while using TEOS-10 [10]. To calculate N^2, we first needed to calculate the Conservative Temperature and Absolute Salinity profiles (again using

TEOS-10). After getting these values, TEOS-10 calculates N^2 by calculating the vertical gradients of these profiles and multiplying them by the acceleration due to gravity, g using Eqn. (3.10.1) of IOC et al. (2010) as follows:

$$g^{-1}N^2 = \alpha^{\Theta}\Theta_z - \beta^{\Theta}\left.\frac{\partial S_A}{\partial z}\right|_{x,y} \tag{2.4}$$

where α^{Θ}, β^{Θ}, Θ and S_A refer to thermal expansion coefficient, haline contraction coefficient, conservative temperature, and absolute salinity, respectively.

The linearised QGPV equation is as follows [9]:

$$\frac{\partial}{\partial t}\left[\nabla^2\psi + \frac{\partial}{\partial z}\left(\frac{f_0^2}{N^2}\frac{\partial\psi}{\partial z}\right)\right] + \beta\frac{\partial\psi}{\partial x} = 0 \tag{2.5}$$

From this we can arrive at the following relation which describes the non-rotational vertical structure of the displacements ϕ_n [7]:

$$\frac{\partial^2\phi_n(z)}{\partial z^2} + \frac{N^2(z)}{c_n^2}\phi_n(z) = 0 \tag{2.6}$$

with boundary conditions: $\phi_n = 0$ at $z = 0, H$

where c_n is the eigenvalue of the equation, ϕ_n is the depth-dependent isopycnal displacement for mode-n and $N^2_{(z)}$ is the Brunt–Väisälä frequency.

Equation 2.6 has analytical solutions only for constant buoyancy profiles [11]. However, in the oceans, the buoyancy profiles are never constant, so we used numerical methods to solve this problem.

This is a Sturm-Liouville problem and can be solved easily by simplifying it into an eigenvalue problem. This was achieved by decomposing the first term in Equation 2.6 into a second-order finite difference matrix (incorporating boundary conditions) and a column vector containing the eigenfunctions, ϕ_n. We also decomposed the second term as a diagonal matrix containing the values of N^2 and the column matrix ϕ_n multiplied by $1/c_n^2$. The finite difference matrix was then multiplied by the inverse of a diagonal $N^2_{(z)}$ matrix to get R and Equation 2.6 simplifies to the following:

$$R\phi_n = \lambda\phi_n$$

(2.7)

where $\lambda = -\frac{1}{c_n^2}$.

By solving Equation 2.7, we could obtain the values of the eigenfunctions, ϕ_n, and the vertical modes associated with the motion and the ratio between the SLA and η. The ratio is as follows:

$$\frac{a_n}{\eta_n(z)} = \frac{c_n^2}{g} \frac{\frac{d\phi_n}{dz}|_0}{\phi_n(z)} \tag{2.8}$$

Here, a_n and $\eta_n(z)$ are the surface displacement and vertical isotherm displacement at a depth of 1000 dbar, respectively, as predicted by Equation 2.6. A more detailed description of the derivation to arrive at Equation 2.8 can be found in Geoffroy and Nycander, 2022 [7].

Chapter 3

Results and Discussion

In this chapter, we look at a few cases where the Argo floats in conjunction with the SLA time series, capture the anti-correlation caused by baroclinic eddies very well and then dive into what this entails. We will first discuss how we identified eddies in the η and SLA time series, giving us an idea of what to expect. Then, we will discuss the vertical eigenmodes that we calculated according to the stratification profiles of the ocean. We will then go on to discuss the results of trying to predict the η time series at 1000 dbar, using the eigenfunctions of Equation 2.6 and the corresponding stratification profile. We also try to look at what kinds of eddies these instances of high correlation correspond to and how long each of them lasts via eddy tracking.

3.1 Correlating SLA and Observed Displacement at 1000 dbar

During the initial analysis, we created a time series of SLA along the tracks of an Argo float for all the floats that fit the criteria in Section 2.2.1. We used these SLA time series and the η time series and then looked for any persistent instances of anti-correlation by calculating the correlation coefficient and the slope for an SLA vs Observed displacement at 1000 dbar graph (shown in Fig 3.2). This gave us an idea of where and when we can expect eddies. This was also useful in identifying which kind of eddy to expect, as Cyclonic

and Anti-Cyclonic eddies have the opposite expression in terms of SLA and η displacement. In Fig 3.1, we have an Argo float in the Indian Ocean, which has good examples of correlation between the two time series. We can see instances of both cyclonic and anti-cyclonic eddies in this.

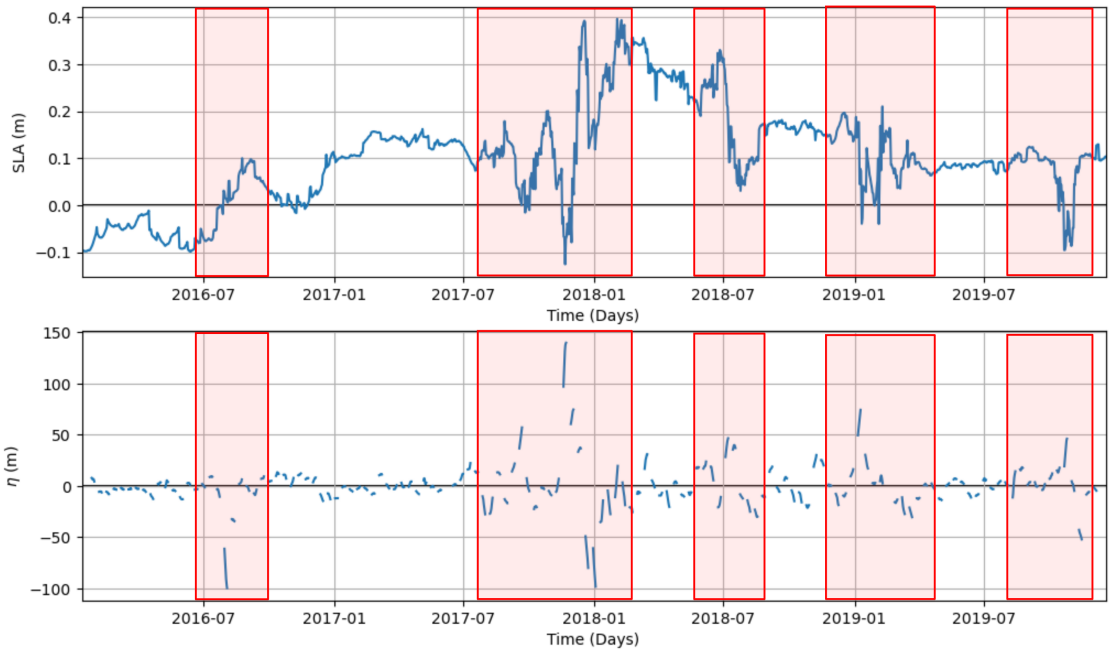

Figure 3.1: The daily SLA time series (above) and the time series of displacement observed by Argo float 5904675 (WMO) at 1000 dbar with periods of high correlation marked by red boxes

3.2 Vertical Modes

We begin by looking at calculated vertical eigenmodes and what they imply.

After solving the Eigenvalue Problem described in Section 2.2.4 according to the boundary conditions, we get a set of eigenvalues and eigenfunctions. The eigenvalues c_n are the phase speed of long mode-n gravity waves in a non-rotating continuously stratified fluid [8] and can be used to calculate the Rossby Radius of Deformation for mode-n at a particular latitude. The Rossby Radius of Deformation (especially mode-1) can determine the size of an eddy at different latitudes. However, the eigenfunctions, $\phi_n(z)$ form a complete set of orthonormal vectors that can be used to predict the surface expression of baroclinic eddies

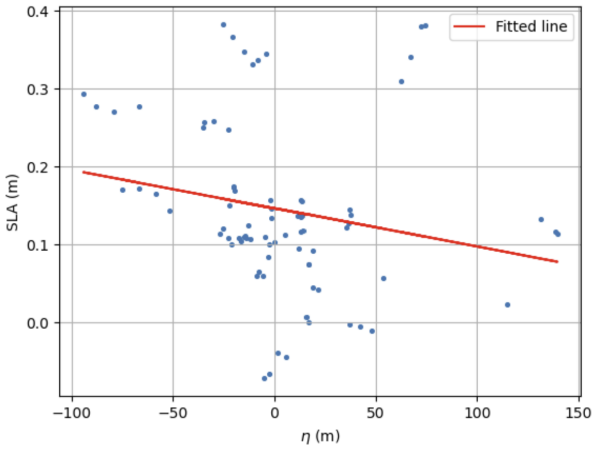

Figure 3.2: Scatter plot of daily SLA time series (above) and the time series of displacement observed by Argo float 5904675 (WMO) from the second period of high correlation in Fig 3.1

(and other phenomenon like internal tides [7]). The eigenfunctions vary with depth to give us sinusoidal curves (Fig. 3.3b & c), and these depth-varying curves can be used to calculate both the surface expression of eddies and also the amplitude of displacement caused by them throughout the depth of the ocean. We can see this mathematically by looking at the ratio described in Equation 2.6.

For mesoscale eddies, we assume most of the SSH variability and variability of isopycnals in the interior correspond to the first baroclinic mode (which is mode-1 here)
[3].

For an constant N^2 profile (as in Fig 3.3(a)), the ordinary differential equation 2.6 can be solved analytically. We used this to validate our code before moving on to real N^2 profiles. The analytical solution says that the ratio between the surface perturbation and the perturbation at a depth in the ocean is as follows:

$$\frac{a_n}{\eta(z)} = \frac{N^2 H}{g\pi} \tag{3.1}$$

where H is the total depth of the water column, and g is the acceleration due to gravity.

From this equation, the ratio implied that for a perturbation of 1 cm at the surface, there should be a perturbation of 10 m at the depth with the maximum mode-1 eigenfunction.

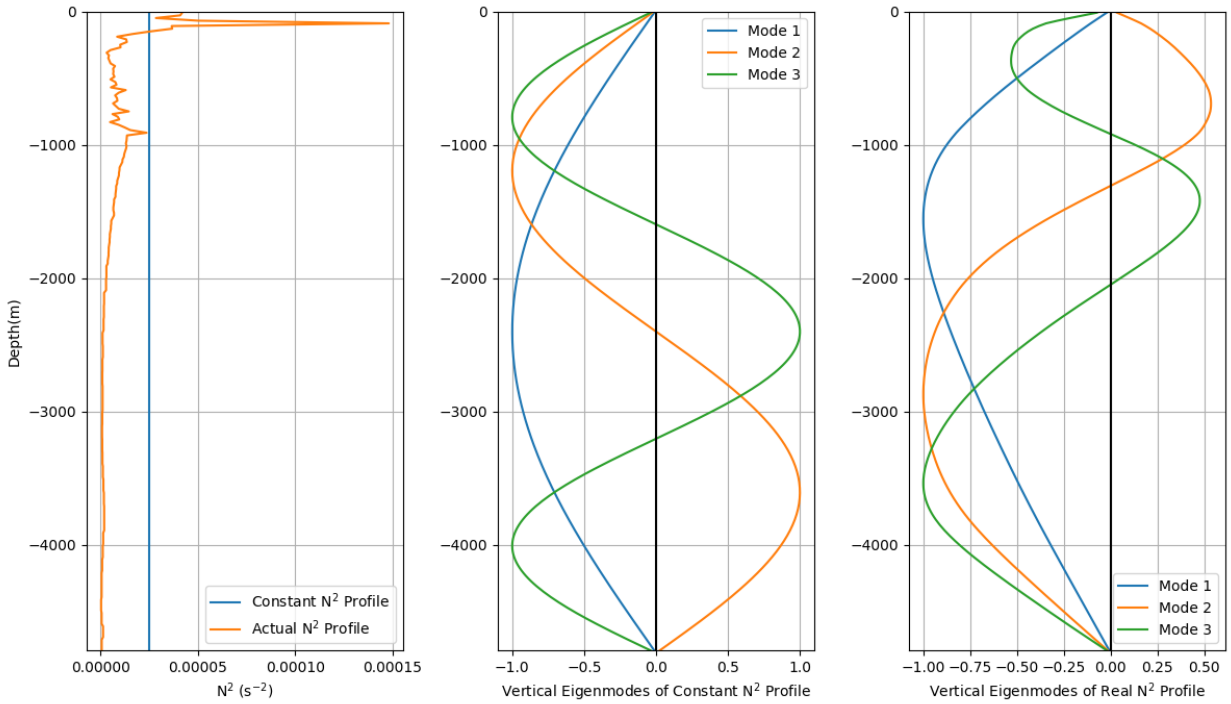

Figure 3.3: (left, a) Stratification profiles: one is an artificial constant buoyancy profile (blue), and the other is a profile from a float in the Indian Ocean (1900411 (WMO)); (middle, b) the normalised vertical eigenmodes for the constant stratification case; (right, c) the normalized vertical eigenmodes for the stratification from the Argo float (1900411 (WMO))

This is close to the expected ratio based on [9], thus validating our code for the artificial case.

For the real cases (like Figs 3.4 - 3.7), we need to solve Equation 2.6 numerically as the N^2 profile changes with depth. The method for this is described in Section 2.2.4. The eigenfunctions we obtain are skewed near the top of the ocean due to the rapid changes in stratification near the surface. The ratios calculated using these values imply a perturbation of 7-9 m at a depth of 1000 dbar for a 1 cm perturbation at the surface. This is better seen in Figs 3.4 and 3.5, where we take the entire SLA time series for a float and the ratio from Equation 2.8 for all the dates when the float took profile measurements and calculated the predicted η time series. The predicted η time series does not match with the actual η time series for the most part, except in certain time periods where we already expect an eddy to be present due to the anti-correlation evident in the SLA and η time series in Fig 3.1. Most of the regions of high anti-correlation in Fig 3.1 can be identified in Fig Fig 3.4, with the exception of one where the amplitude is not high enough for the

predicted time series to coincide with the observed displacement (this point is also not validated by the AVISO data in section 3.4).

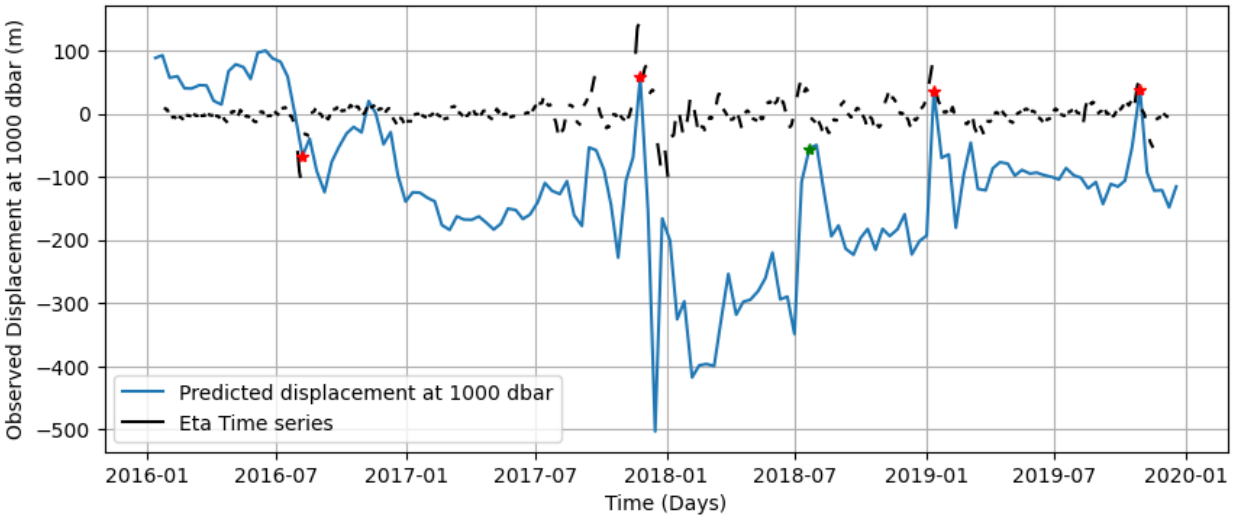

Figure 3.4: The η time series for float 5904675 (WMO) in black, with the displacement predicted by the first Baroclinic mode in blue. Points, where both curves coincide, are marked by red stars; the green star depicts a point where we expected the curves to coincide.

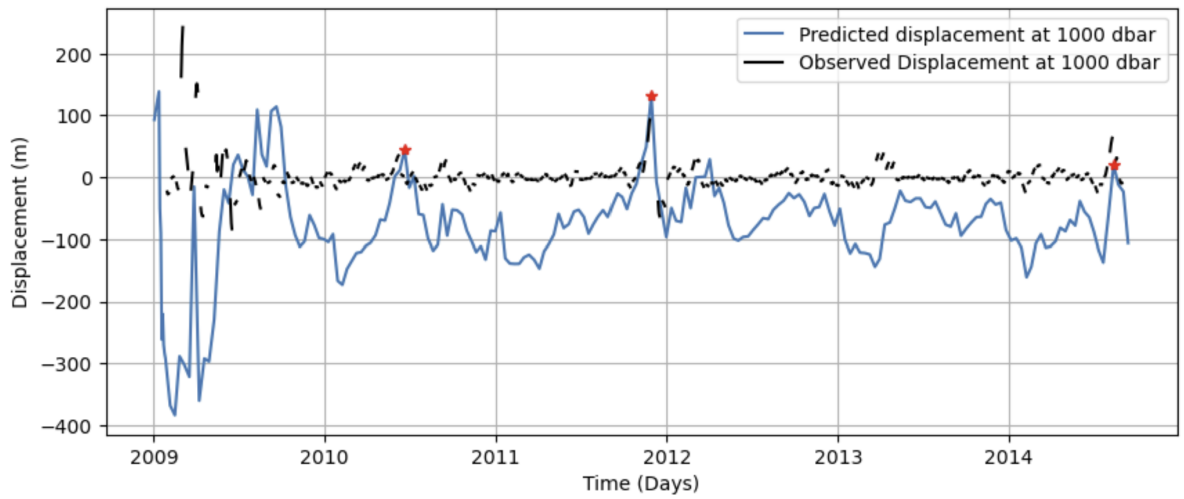

Figure 3.5: The η time series for float 5902105 (WMO) in black, with the displacement predicted by the first Baroclinic mode in blue.

This implies that our Eigenvalue Problem code is accurately capturing eddies and much of the amplitude of the displacement they cause at 1000 dbar. The parts of the time series that don't correlate well (the entirety of Figs 3.6 and 3.7) can be explained as not having

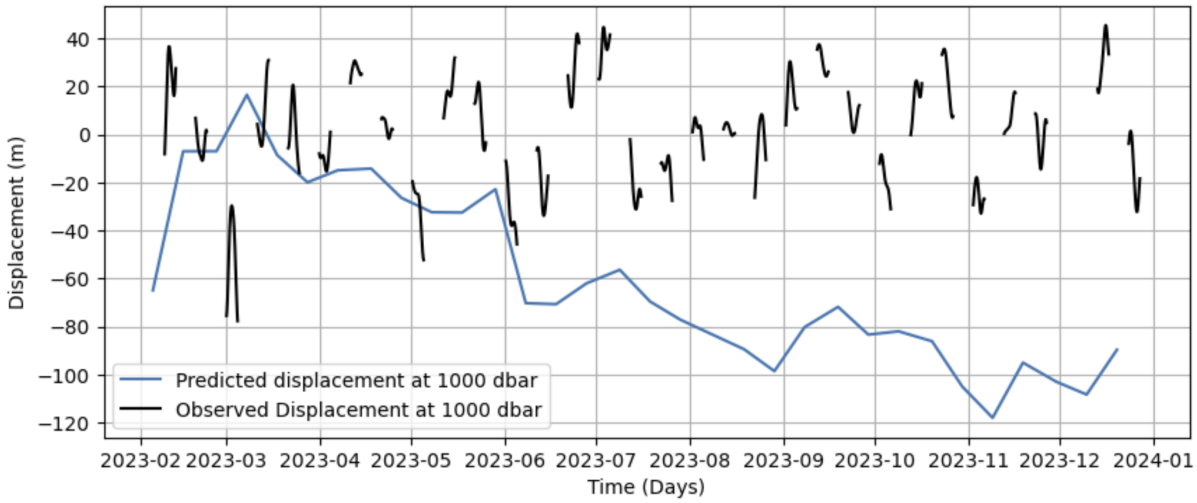

Figure 3.6: The η time series for float 3902368 (WMO) in black, with the displacement predicted by the first Baroclinic mode in blue.

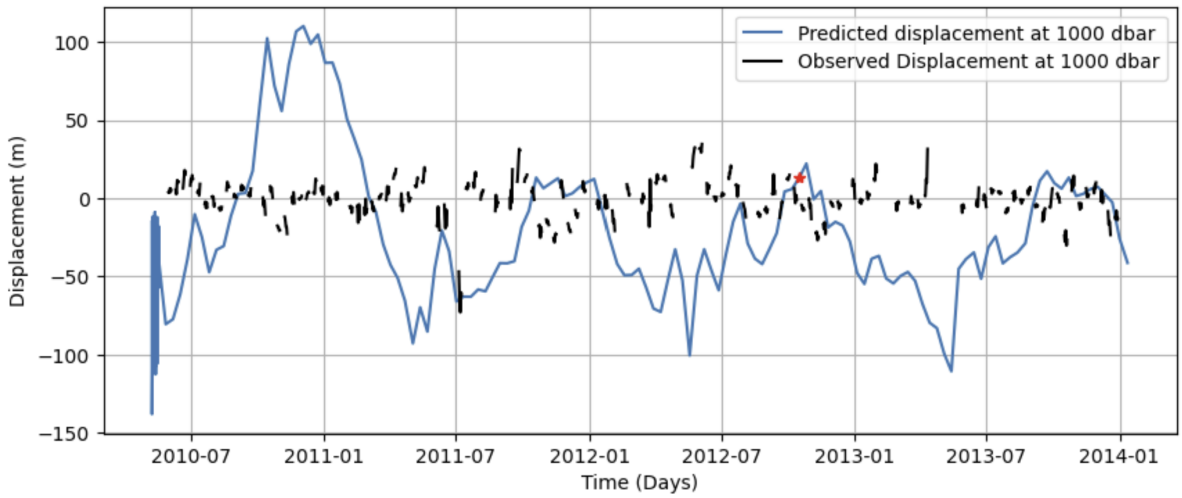

Figure 3.7: The η time series for float 5902266 (WMO) in black, with the displacement predicted by the first Baroclinic mode in blue.

much noticeable eddy activity or having influence from higher modes. Additionally, the predicted η time series has a slightly lower amplitude than the actual η time series in most cases. This can be due to a multitude of reasons. The boundary conditions we have chosen to solve for in Equation 2.4 assume a rigid lid at the top and imply a flat bottom, ignoring any bottom topography and, hence, the vertical velocities as well. While this might be a reasonable assumption in the open ocean, it leaves much to desired near the continental

slopes.

3.3 Eddy Tracking

We used the AVISO data set to confirm the presence of the eddies that we detected using the SLA and η time series. This data set provided us with the trajectories of the eddies that an Argo float encounters. We can then observe these eddies from their inception till dissipation and not just when they encounter the Argo float. There are also sometimes more eddies that a float may encounter than what we see in the SLA and η time series. We can then use the AVISO data set to look at the characteristics of the eddies that we couldn't detect and maybe make changes to our methods. This part of the project is still underway.

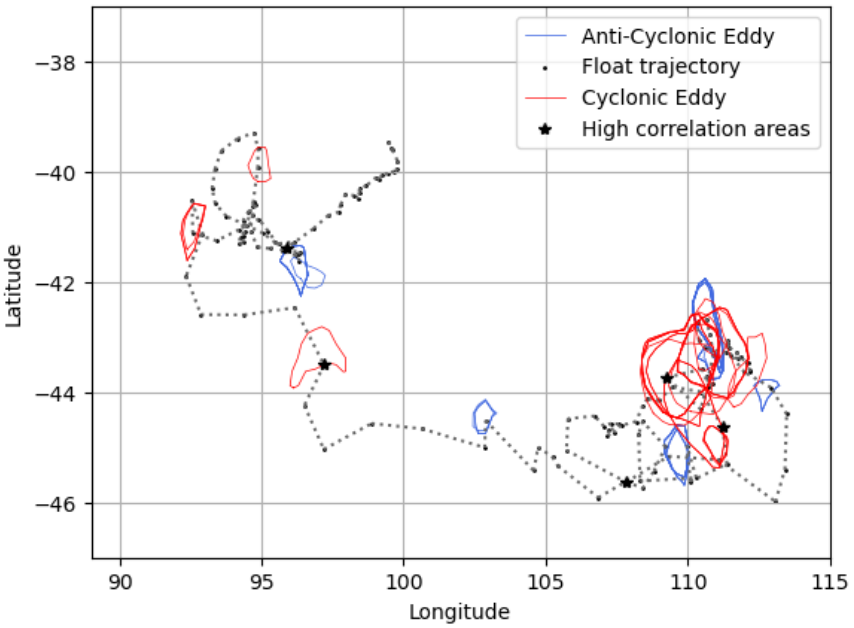

Figure 3.8: The blue contours are anti-cyclonic eddies, and the red ones are cyclonic eddies from the AVISO data set, the black stars represent the high correlation areas from Fig 3.1, the black line is the float trajectory for float 5904675 (WMO). 1-5 correspond to the high correlation areas in Fig 3.1.

Fig 3.8 shows one example of all the eddies that a float has passed through during its lifetime. Not all of these show up in Fig 3.1 or Fig 3.4, which could be due to a multitude

of reasons ranging from the resolution of the SLA data set being too coarse to detect smaller eddies, or maybe they barely passed by the float.

3.4 Future Directions

Now that we have this global data set of Argo floats where we can accurately detect eddies, we can look at instances where there is no correlation or even positive correlation more deeply. The important thing to focus on first would be to make more of the Argo data we have usable by perhaps changing the filtering techniques. This would give us a much bigger data set to use, which will be crucial for any future global studies. We also intend to explore the different boundary conditions (similar to those in [3]) to see if that decreases the difference in amplitude between the predicted and observed η time series. We also plan to use higher-resolution SLA data to create even more accurate SLA time series along the track of the float. We also aim to see how much of the latitudinal variability can be captured in the Argo park phase data and how different properties of eddies change in different ocean basins. Another thing we plan to explore is the cause of some floats having a high positive correlation between the surface and η time series instead of high anti-correlation.

Chapter 4

Conclusion

In this thesis project, we explored using the Argo Park Phase data set to examine mesoscale ocean eddies. Using the park phase data, we could make a time series of vertical displacement of isotherms and watch them move due to the influence of eddies. Eddies have been studied extensively using satellite measurements, shipboard and buoy measurements, but the park phase data allows us to look at eddies with a lot of accuracy with only a simple procedure for recognising eddies.

Our main and most important result is that the correlation between the Argo park phase detected eddies and the eddies predicted by the eigenvalue problem solution is very good in some of the cases we have studied so far. We can also see these park phase eddies in AVISO data, which is obtained from satellite data as well. This is great as identifying eddies from Argo data was relatively easy and used less extra data like the eigenvalue problem or computational time, like the AVISO data.

There are some issues with our approach as well. The Argo data doesn't seem to catch all the eddies it passes through. The amplitude of the displacement at 1000 dbar predicted by the Eigenvalue Problem solution is slightly different from the one we expect from the Argo η time series.

So far, in this project, we have focused on building these different methods of detecting and validating eddies. Now, we intend to use this data set to look into how much of the variation caused by large-scale phenomena described earlier can be seen by each approach.

Appendix

Deriving the Vertical Structure Eigenvalue Equation from the QGPV Equation

The QGPV equation in terms of stream functions is as follows [12]:

$$(\frac{\partial}{\partial t} + u\frac{\partial}{\partial x} + v\frac{\partial}{\partial y})[\nabla^2\psi + \frac{\partial}{\partial z}\frac{f_0^2}{N^2}\frac{\partial\psi}{\partial z} + \beta y] = 0 \tag{4.1}$$

where all symbols have their usual meanings.

Expanding this equation, we get:

$$\frac{\partial}{\partial t}[\nabla^2\psi + \frac{\partial}{\partial z}(\frac{f_0^2}{N^2}\frac{\partial\psi}{\partial z})] + \frac{\partial\psi}{\partial x}\frac{\partial}{\partial y}[\nabla^2\psi + \frac{\partial}{\partial z}(\frac{f_0^2}{N^2}\frac{\partial\psi}{\partial z})] - \frac{\partial\psi}{\partial y}\frac{\partial}{\partial x}[\nabla^2\psi + \frac{\partial}{\partial z}(\frac{f_0^2}{N^2}\frac{\partial\psi}{\partial z})] + \beta\frac{\partial\psi}{\partial x} = 0 \tag{4.2}$$

To linearise this equation, we lose the non-linear advection terms (the second and third terms in Equation 4.2). After this, the equation becomes,

$$\frac{\partial}{\partial t}[\nabla^2\psi + \frac{\partial}{\partial z}(\frac{f_0^2}{N^2}\frac{\partial\psi}{\partial z})] + \beta\frac{\partial\psi}{\partial x} = 0 \tag{4.3}$$

This is the linearized Quasi-Geostrophic Potential Vorticity Equation.

Assuming Equation 4.3 has solutions of the form: $\psi(x,y,z,t) = \Phi(z).\Psi(x,y,t)$ and then substituting this into Equation 4.3, we get:

$$\frac{\partial}{\partial t}\left[\Phi(z)\nabla^2\Psi + \frac{d}{dz}\left(\frac{f_0^2}{N^2(z)}\frac{d\Phi(z)}{dz}\Psi\right)\right] + \beta\Phi(z)\frac{\partial\Psi}{\partial x} = 0$$

Taking in the time derivative, we get,

$$\Phi(z)\left[\nabla^2\frac{\partial\Psi}{\partial t} + \beta\frac{\partial\Psi}{\partial x}\right] + \left(\frac{d}{dz}\left(\frac{f_0^2}{N^2(z)}\frac{d\Phi}{dz}\right)\right)\frac{\partial\Psi}{\partial t} = 0$$

Assuming wave-like solutions for the horizontal part [3],

$$\Psi(x,y,t) = e^{i(kx+ly-\omega t)}$$

Substituting this into the equation:

$$\Phi(z)\left[-i\omega(-(k^2+l^2)) + i\beta k\right]\Psi - i\omega\left(\frac{d}{dz}\left(\frac{f_0^2}{N^2}\frac{d\Phi}{dz}\right)\right)\Psi = 0$$

Cancel $i\omega\Psi$ (assuming $\omega \neq 0$):

$$\Phi(z)\left[(k^2+l^2) - \frac{\beta k}{\omega}\right] = \frac{d}{dz}\left(\frac{f_0^2}{N^2(z)}\frac{d\Phi}{dz}\right)$$

Let

$$\lambda^2 = -[(k^2+l^2) + \frac{\beta k}{\omega}]$$

where λ ([3]) is the eigenvalue of Equation 4.4. This simplifies to,

$$\frac{d}{dz}\left(\frac{f_0^2}{N^2(z)}\frac{d\Phi}{dz}\right) + \lambda^2\Phi(z) = 0 \tag{4.4}$$

Now, let $\phi = \frac{f_0^2}{N^2}\frac{d\Phi}{dz}$. Substituting this into Equation 4.4, we get:

$$\frac{d\phi}{dz} + \lambda^2\Phi(z) = 0$$

Differentiating this equation with respect to z, we get:

$$\frac{d^2\phi}{dz^2} + \lambda^2\frac{d\phi(z)}{dz} = 0$$

Substituting ϕ again into this equation, we get:

$$\frac{d^2\phi}{dz^2} + \frac{N^2}{c^2}\phi = 0 \tag{4.5}$$

where $c = \frac{f_0}{\lambda}$.

The boundary conditions of Equation 4.5 now become $\phi = 0$ at $z = 0, H$.

This is the Sturm-Liouville Eigenvalue problem that we solve in Section 2.2.4.

Bibliography

[1] D. B. Chelton, M. G. Schlax, R. M. Samelson, and R. A. de Szoeke, "Global observations of large oceanic eddies," *Geophysical Research Letters*, vol. 34, no. 15, 2007.

[2] J. K. McWhorter, H. L. Roman-Stork, M. Le Hénaff, H. Frenzel, M. A. Johnston, M. Cornec, and E. Osborne, "Mesoscale Eddies Influence Coral Reef Environments in the Northwest Gulf of Mexico," *Journal of Geophysical Research: Oceans*, vol. 129, no. 6, p. e2023JC020821, 2024. _eprint: https://onlinelibrary.wiley.com/doi/pdf/10.1029/2023JC020821.

[3] M. S. de La Lama, J. H. LaCasce, and H. K. Fuhr, "The vertical structure of ocean eddies," *Dynamics and Statistics of the Climate System*, vol. 1, p. dzw001, 09 2016.

[4] C. Wunsch, "The vertical partition of oceanic horizontal kinetic energy," *Journal of Physical Oceanography*, vol. 27, no. 8, pp. 1770 – 1794, 1997.

[5] D. Roemmich, G. C. Johnson, S. Riser, R. Davis, J. Gilson, W. B. Owens, S. L. Garzoli, C. Schmid, and M. Ignaszewski, "The Argo Program: Observing the Global Ocean with Profiling Floats," *Oceanography*, vol. 22, no. 2, pp. 34–43, 2009. Publisher: Oceanography Society.

[6] T. D. Hennon, S. C. Riser, and M. H. Alford, "Observations of Internal Gravity Waves by Argo Floats," *Journal of Physical Oceanography*, vol. 44, pp. 2370–2386, Sept. 2014.

[7] G. Geoffroy and J. Nycander, "Global mapping of the nonstationary semidiurnal internal tide using argo data," *Journal of Geophysical Research: Oceans*, vol. 127, no. 4, p. e2021JC018283, 2022. e2021JC018283 2021JC018283.

[8] D. B. Chelton, R. A. deSzoeke, M. G. Schlax, K. E. Naggar, and N. Siwertz, "Geographical variability of the first baroclinic rossby radius of deformation," *Journal of Physical Oceanography*, vol. 28, no. 3, pp. 433 – 460, 1998.

[9] A. Gill, *Atmosphere-Ocean Dynamics*. No. v. 30 in Atmosphere-Ocean Dynamics, Elsevier Science, 1982.

[10] S. Ioc, "The international thermodynamic equation of seawater–2010: Calculation and use of thermodynamic properties," *Intergovernmental Oceanographic Commission, UNESCO Manuals and Guides No*, vol. 56, no. 203, p. 196, 2010.

[11] G. K. Vallis, *Atmospheric and oceanic fluid dynamics*. Cambridge University Press, 2017.

[12] J. R. Holton and G. J. Hakim, eds., *An Introduction to Dynamic Meteorology (Fifth Edition)*. Boston: Academic Press, fifth edition ed., 2013.